

DEVIATIONS FROM RAYLEIGH STATISTICS IN ULTRASONIC SPECKLE

T.A. Tuthill, R.H. Sperry and K.J. Parker

University of Rochester
Rochester, NY 14627

The statistics of speckle patterns in ultrasound images have potential for tissue characterization. In "fully developed speckle" from many random scatterers, the amplitude is widely recognized as possessing a Rayleigh distribution. This study examines how scattering populations and signal processing can produce non-Rayleigh distributions. The first order speckle statistics are shown to depend on random scatterer density and the amplitude

Key words: Rayleigh statistics; scatterer populations; simulations; speckle; system effects; tissue characterization.

I. INTRODUCTION

The propagation of ultrasound in parenchymal tissue is fundamentally a statistical process, and numerous tissue characterization techniques are based on this concept. Both the radio frequency (RF) and envelope signals of in B-scans of liver parenchyma, the image texture has been compared to laser

provides information, as the second order statistics are governed by the system's resolution. The speckle also reduces lesion contrast detection and, consequently, has sometimes been minimized by compounding [4] or filtering [5]. Yet, the liver stroma is comprised of lobules constructed about central veins and bordered by portal triads [6]; thus, "structure" has been suggested as a cause of non-Rayleigh statistics. First order statistics, such as the signal-to-noise ratio (SNR), have been used as discriminators in liver [7] and cardiac [8,9] studies. Assuming the presence of periodic scatterers, the mean spacing

This report is concerned only with first order statistics in an attempt to better understand the physical causes for the various observed statistical parameters. It begins with simple acoustic models for generating Rayleigh and non-Rayleigh distributions, and demonstrates artifacts which can result

II. THEORY

The derivations for Rayleigh and Rician distributions are given in Middleton [1] and outlined below. For multiple random reflections in a sample volume, the received echo is a random signal

$$s(t) = x(t)\cos(\omega_0 t) - y(t)\sin(\omega_0 t) \quad (1)$$

where ω_0 is the center frequency, and the quadrature components $x(t)$ and $y(t)$ are independent and zero-mean Gaussian. The calculated envelope $r(t)$ may be expressed by the quadrature components

$$r(t) = \sqrt{x^2(t) + y^2(t)} \quad (2)$$

or by a sum using the Hilbert transform $\hat{s}(t)$

$$r(t) = |s(t) + j\hat{s}(t)| \quad (3)$$

$$p_r(r) = \frac{r}{\sigma^2} e^{-r^2/2\sigma^2} \quad (4)$$

where σ^2 is the variance of the quadrature components, and the signal-to-noise ratio is a constant,

$$\text{SNR} = \frac{\langle r \rangle}{\sigma} = 1.91 \quad (5)$$

For the case of few scatterers per sample volume, the speckle is not fully developed and has a lower (<1.9) SNR. The distribution is then termed pre-Rayleigh.

If an additional signal (due possibly to "structure" or periodic scatterers),

$$s'(t) = A(t)\cos(\omega_0 t + \theta(t)) \quad (6)$$

is combined with a Rayleigh RF signal, the revised distribution has the form

$$p_r(r) = \frac{r}{\sigma^2} e^{-[r^2 + A^2(t)]/2\sigma^2} I_0\left[\frac{A(t)r}{\sigma^2}\right] \quad (7)$$

where $I_0(\)$ is the modified Bessel function. If $A(t)$ is constant, the distribution is labeled Rician, a term used in optics to describe laser speckle in the presence of a coherent background with constant intensity [3].

III. EFFECTS OF SCATTERER DENSITIES

Gaussian-enveloped pulse with center frequency 2.5 MHz and a -6dB bandwidth of 0.04 MHz. In this simulation, the Gaussian envelope had a

rate was 30 MHz. Scatterers were modeled by discrete reflectors of random

convolving the pulse with a scattering train to form a 2000 point waveform analogous to 5 cm of tissue. Each analysis used ten independent lines, corresponding to a large region of interest in a tissue scan. The envelopes were calculated using the Hilbert transform in the frequency domain, and histograms were computed from the ten scan lines.

a) Random Scatterers

The initial study looked at the effects of scatterer density as described by the number of scatterers per pulse width, ranging from sparse to densely packed. The sparse reflector densities give pre-Rayleigh distributions with low SNRs, a result previously noted by Oosterveld [20]. Figure 1a shows a scan line for 2 scatterers/ ΔT , along with its analytic envelope. In this and subsequent examples, a histogram curve fit is obtained from the maximum likelihood estimate for a Rayleigh distribution [21], $\sigma^2 = (\Sigma r^2)/2N$, where N is the number of samples. In figure 1b, the curve fit (dotted line) is shown to deviate from the envelope histogram. As the density increases, the histograms approach Rayleigh distributions. For five or more scatterers/ ΔT (a typical scan line is shown in figure 2a), the SNR remains at 1.9 ± 0.1 (Fig. 2b).

b) Bimodal Populations

A possibly more realistic modeling of liver parenchyma involves bimodal distributions, formed by adding different classes of scatterers to the densely packed case. The effects of amplitude spacing and periodicity were strong scatterers superimposed on a train of dense random scatterers which

amplitude of the random scatterers.

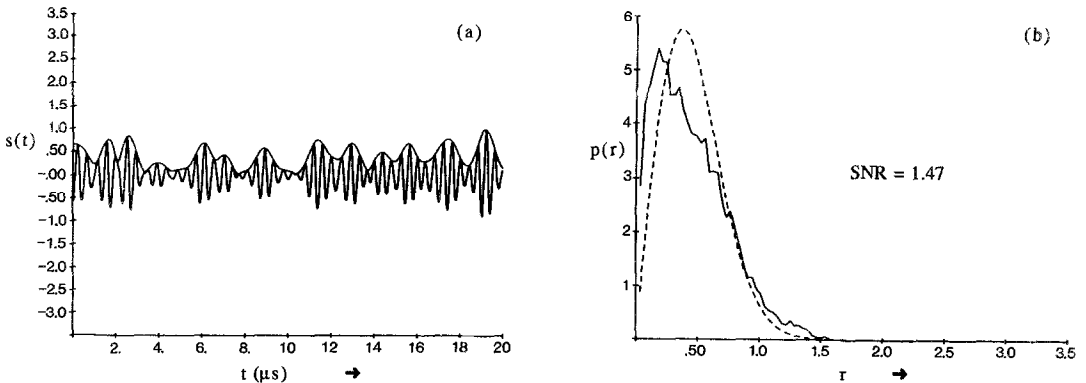


Fig. 1 a) Simulated RF signal for sparse scatterers (2 scatterers/ ΔT) and analytic envelope. b) Corresponding envelope histogram with Rayleigh curve fit (dotted line).

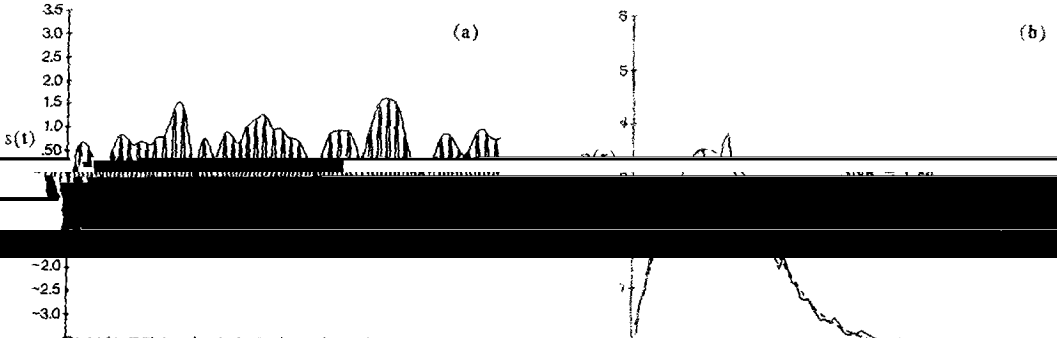


Fig. 2. a) Estimated signal for dense scatterers (σ scatterers/ Δr) and analytic envelope. b) Corresponding envelope histogram with

For strong, sparse scatterers, simulating occasional small arteries in tissue, the envelope distribution appears pre-Rayleigh (Fig. 3), and the SNR drops below 1.9. This addition of occasional strong scatterers causes a wider variation in amplitudes and an increase in σ that is larger than the increase in μ , so that the SNR decreases. In contrast, for strong periodic scatterers,

However, as the spacing of the strong periodic scatterers is decreased to the extent where they become subresolvable, the distributions are highly dependent on the ratio of the periodic scatterer spacing to the wavelength. This concept is similar to the Bragg condition in X-ray diffraction. With spacings close to an integral number of wavelengths, returning echoes interfere constructively, providing a dominant signal. Here again, the SNR is

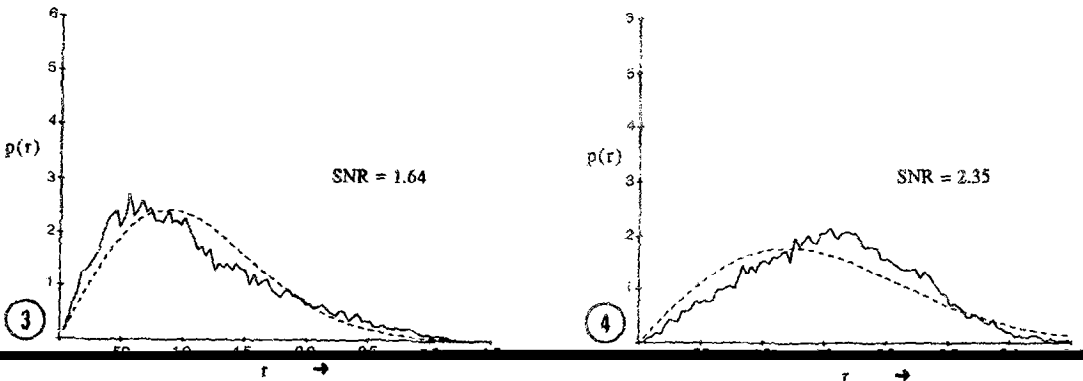


Fig. 3 Envelope histogram for bimodal scatterer distribution of sparse scatterers with dense random scatterers (dotted line is Rayleigh curve fit).

Fig. 4 Envelope histogram for bimodal scatterer distribution of strong periodic, just resolvable scatterers with dense random scatterers (dotted line is Rayleigh curve fit).

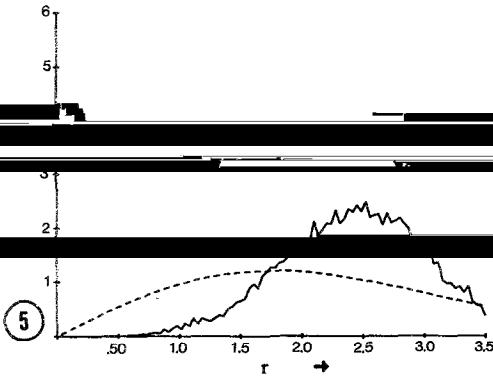


Fig. 5 Envelope histogram for bimodal scatterer distribution of dense random scatterers and strong, periodic, subresolvable scatterers with integral wavelength spacing (dotted line is Rayleigh curve fit).

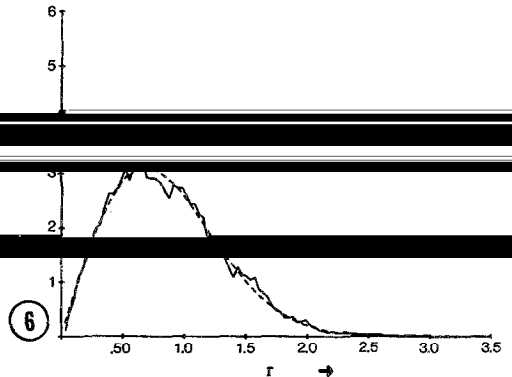


Fig. 6 Envelope histogram for bimodal scatterer distribution of dense random scatterers and strong, periodic, subresolvable scatterers with spacing of an odd number of half-wavelengths (dotted line is Rayleigh curve fit).

greater than 1.9, and the distribution is Rician-like (Fig. 5). As the scatterer spacing approaches an odd number of half-wavelengths, the SNR drops to 1.9 (Fig. 6). In this case, destructive interference cancels out any effect of the added periodic scatterers, and the distribution is reduced to Rayleigh.

Figure 7 summarizes the equivocal relationship between periodic

greater than a pulsewidth, the SNR remains below 1.9. The addition of 10 percent amplitude and spacing jitter to the periodic scatterers decreases the SNR for large spacings (dashed line). A reduction in the amplitude of the periodic scatterers has a similar effect.

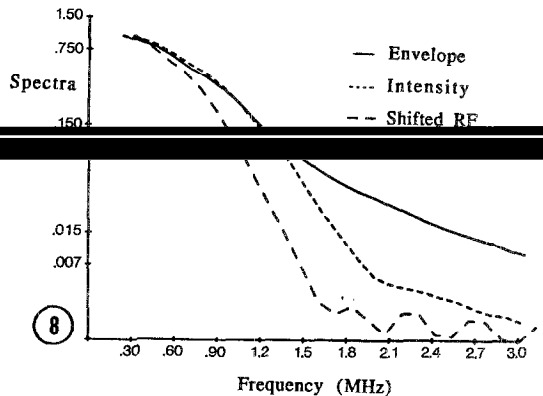
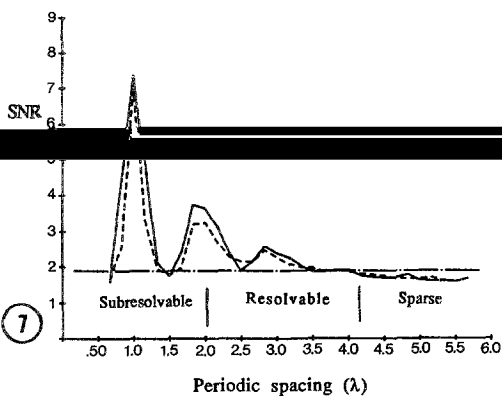


Fig. 7 Plot of SNR vs. periodic scatterer spacing. Dotted line shows effects from adding 10 percent amplitude and spacing jitter.

spectrum shifted to 0) for dense random scatterers.

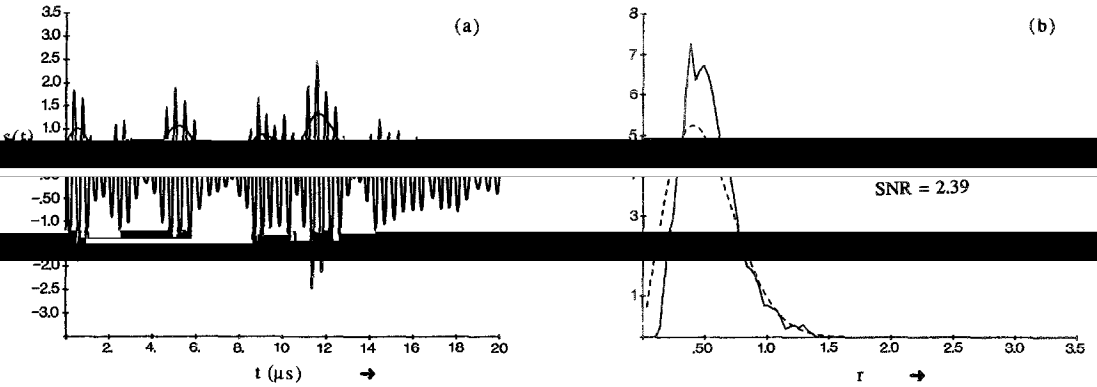


Fig. 9 a) Simulated RF signal for dense scatterers, and low pass filtered (1 MHz width) envelope. b) Corresponding envelope histogram with Rayleigh curve fit (dotted line).

IV. SYSTEM EFFECTS

a) Envelope Detection

filtering the data. For a bandlimited RF signal, quadrature components will be

nonlinear step (positive square root in Eq. (2)) in processing, which generally results in the production of higher harmonics. Figure 8 shows the normalized amplitude spectra of a typical scan line, its intensity, and its envelope. The envelope is shown to have a wider bandwidth than the intensity. To examine the effects of filtering on the histograms, the dense scatterer RF signal was rectified and low-pass filtered with varying width Blackman filters. Using a 1 MHz lowpass filter, the envelope shows smoothed peaks and filled valleys (Fig. 9). The corresponding distribution appears shifted with a high SNR. As the

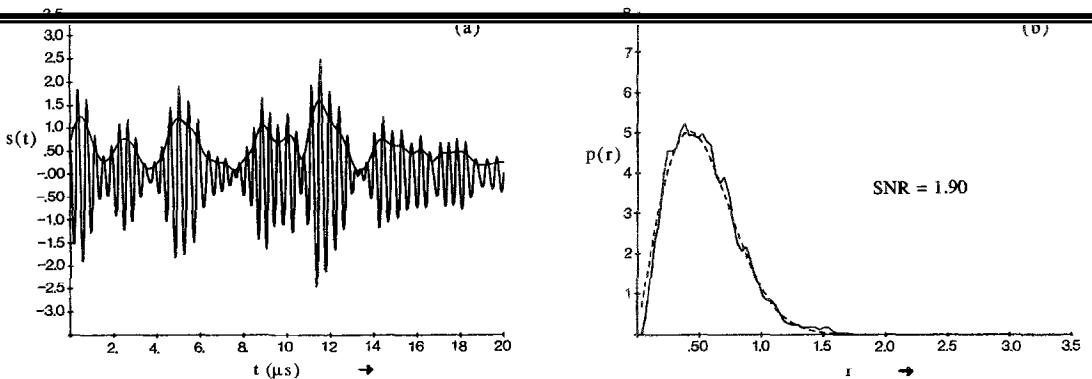


Fig. 10 a) Same RF signal as 9a, but envelope determined with 4 MHz low pass filter. b) Corresponding envelope histogram with Rayleigh curve fit (dotted line).

Fig. 11 Actual liver scan using Octoson with envelope histogram (inset) of blocked region. SNR = 2.71

Fig. 12 Decompressed image of figure 11 with envelope histogram (inset) of blocked region. SNR = 1.53

b) Log Amplification

Amplifier effects on the envelope distribution were also examined for actual clinical data. Using a liver scan obtained from the Octoson with 10 MHz sampling a region was chosen with area comparable to that used in the

displays a Rician-like distribution.

By decompressing the data (relinearizing using calibration data as outlined by Parker and Waag [23]), the histogram approaches Rayleigh, as shown in figure 12. The SNR is lower than 1.9 here due to the high amplitudes from the few strong specular scatterers included in the region of interest. This section of the liver would correspond to the bimodal model of figure 3, with fully developed speckle plus areas of strong reflectors.

The simulations in section III are ideal cases in that the pulses are Gaussian and no attenuation or noise is present. To examine speckle statistics for more "realistic" scan lines, the RF signal was modified slightly. With the application of a wideband nonsymmetric pulse, the SNR decreased less than 10 percent for Rayleigh and periodic resolvable scatterers, and the subresolvable

approximate value for liver tissue at 2.5 MHz, the SNRs were reduced by about 5 to 20 percent for Rayleigh and resolvable scatterers and by up to 60 percent for subresolvable. Since most scanners have some gain compensation, a lower attenuation coefficient (0.035 np/cm) was also examined and shown to have negligible effects. Finally, changing the bandwidth of the Gaussian pulse did not affect the previous results as long as the number of scatterers per pulse width was consistent and the relation of the spacing with the wavelength was considered.

VI. CONCLUSIONS

This study shows that there are distinct differences between both Rayleigh and Rician-like distributions. For Rayleigh statistics, at least five random scatterers per pulse width are needed. This limit is comparable to Oosterveld's results [20] if the sample volume is estimated from the reported

population in combination with regularly spaced, high amplitude reflectors

A few guidelines are suggested for performing a statistical analysis. For tissue discrimination, a large region of interest is necessary in obtaining an averaged estimate of the SNR. For our simulations, which use an equivalent of

many, any amplifier nonlinearities should be characterized and removed before proceeding with the analyses.

REFERENCES

- [1] R. W. L. Chan, *IEEE Trans. on Ultrason. Ferroelectr. and Freq. Control*, **36**, 1001-1010 (1988).
- [2] Abbott, J.C. and Thurstone, F.I., *Acoustic speckle and its applications*, pp. 1-10 (1981).
- [3] Goodman, J.W., *Statistical Properties of Laser Speckle Patterns*, in *Laser Speckle and Related Phenomena*, J. C. Dainty, ed., (Springer-Verlag, Berlin, 1975).
- [4] Wells, P.N.T. and Halliwell, M., *Speckle in ultrasonic imaging*, *Ultrasonics* **19**, 225-229 (1981).
- [6] Bockus, H.L., *Gastroenterology* (W.B. Saunders Co. Philadelphia 1965).
- Biological Tissues, in *IEEE Seventh Annual Conference of the Eng. in Med. and Biology Society*, pp. 241-243 (IEEE CH2198-0, 1985).
- [8] Green, S.E., Joynt, L.F., Fitzgerald, P.J., Rubenson, D.S., and Popp, R.L., *In vivo ultrasonic tissue characterization of human liver*, *IEEE Trans. on Ultrason. Ferroelectr. and Freq. Control*, **36**, 1001-1010 (1988).
- [9] Vieli, A., Heiserman, J., Schnittger, I., and Popp, R.L., *An improved stochastic approach to RF amplitude analysis in ultrasonic cardiac tissue characterization*, *Ultrasonic Imaging* **6**, 139-151 (1984).

- [10] Sommer, F.G., Joynt, L.F., Carroll, B.A., and Macovski, A., Ultrasonic characterization of abdominal tissue via digital analysis of backscattered waveforms, *Radiology* 141, 811-817 (1981).
- [11] ... *specimens in vivo, Ultrasonics* 20, 82-86 (1982).
- [12] Fallinber, J.L. and Sommer, F.G., Ultrasonic characterization of tissue *Ultrasonics SU-31*, 418-428 (1984).
- [13] Wagner, R. F., Smith, S.W., Sandrik, J.M., and Lopez, H., Statistics of speckle in ultrasound B-scans, *IEEE Trans. Sonics Ultrasonics SU-30*, 156-163 (1981).
- [14] Smith, S.W. and Wagner, R.F., Ultrasound speckle size and lesion signal *IEEE Trans. Sonics Ultrasonics SU-30*, 154-160 (1981).
- [15] Wagner, R.F., Insana, M.F., and Brown, D.G., Unified approach to the detection and classification of speckle texture in diagnostic ultrasound, *Optical Eng.* 25, 738-742 (1986).
- [16] Insana, M. F., Wagner, R.F., Garra, B.S., Brown, D.G., and Shawker, T.H., Analysis of ultrasound image texture via generalized Rician statistics, *Optical Eng.* 25, 743-748 (1986).
- [17] Wagner, R.F., Insana, M.F., and Brown, D.G., Statistical properties of radio-frequency and envelope-detected signals with applications to medical ultrasound, *J. Opt. Soc. Am.* 4, 910-922 (1987).
- [18] Kuc, R., Ultrasonic tissue characterization using kurtosis, *IEEE Trans.*
- [19] Middleton, D., *Statistical Communication Theory*, (McGraw-Hill, New York, 1960).
- [20] Oosterveld, B.J., Thijssen, J.M., and Verhoef, W.A., Texture of B-mode echograms: 3-D simulations and experiments of the effects of diffraction and scatterer density, *Ultrasonic Imaging* 7, 142-160 (1985).
- [21] ...
- [22] Durrandii, J., Envelope and pre-envelope of real waveforms, *IEEE*
- [23] Parker, K.J. and Waag, R.C., Measurement of ultrasonic attenuation within regions selected from B-scan images, *IEEE Trans. Biomed. Eng. BME-30*, 431-437 (1983).